Spectrochimica Acta Part A: Molecular and Biomolecular Spectroscopy 264 (2022) 120271

Contents lists available at ScienceDirect

Spectrochimica Acta Part A: Molecular and Biomolecular Spectroscopy

journal homepage: www.elsevier.com/locate/saa

Distinguishing normal and inflammatory models by viscosity changes with sensitively mitochondrial-trackable fluorescent probe

Chen Geng, Jingting Zhan, Xinya Hao, Wenhui Song, Weiying Lin *

Guangxi Key Laboratory of Electrochemical Energy Materials, Institute of Optical Materials and Chemical Biology, School of Chemistry and Chemical Engineering, Guangxi University, Nanning, Guangxi 530004, PR China

HIGHLIGHTS

- A new Near-infrared fluorescent probe with minimal molecular weight.
- A large fluorescence enhancement (195-fold) with red emission.
- A large Stokes shift (160 nm) and excellent biocompatibility in PBS.
- Mitochondrial targeting capabilities and live imaging of small animals.

GRAPHICAL ABSTRACT

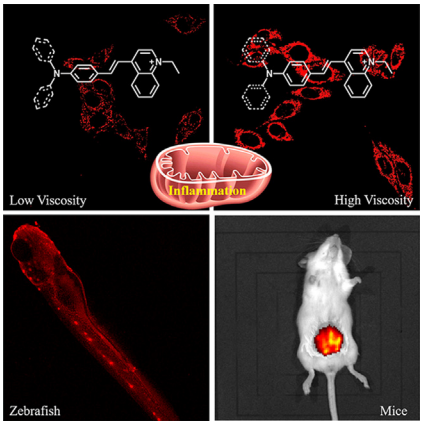

ARTICLE INFO

Article history:
Received 1 July 2021
Received in revised form 2 August 2021
Accepted 7 August 2021
Available online 13 August 2021

Keywords:
Fluorescent probe
Viscosity
Mitochondrial
Inflammation

ABSTRACT

Biological microenvironment plays a momentous role in the regulation of various vital activities, and its abnormal changes are often closely related to some diseases. Viscosity, as an indispensable part of microenvironment parameters, has always been one of the research hotspots of investigators. Herein, we constructed a new red-emitting fluorescent probe (**HVM**) to identify the abnormal situation of mitochondria through viscosity changes in the biological microenvironment. Interestingly, **HVM** has excellent optical properties such as large stokes shift (160 nm), viscosity sensitivity (195-fold), high photostability, and biochemical properties with low cytotoxicity and excellent biocompatibility. For these reasons, the novel probe could successfully be used to identify the normal and inflammatory models via viscosity changes in biological experiments. Therefore, we provided a convenient synthetic route to obtain viscosity sensor **HVM** with excellent application properties.

1. Introduction

Cell viscosity, an important microenvironment parameter, is a significant factor affecting macromolecular interaction, chemical signal transmission and active metabolite diffusion in living cells [1–5]. Abnormal changes of viscosity associated with dysfunction and clinical symptoms, including diabetes, hypertension, atherosclerosis, cancer and so on [6–9]. Therefore, monitoring cell viscosity is become an effective means to distinguish normal cells from inflammatory cells. As a kind of semi-autonomous organelle, mitochondria play an indispensable role in multitudinous life

* Corresponding author.
E-mail address: weiyinglin2013@163.com (W. Lin).

https://doi.org/10.1016/j.saa.2021.120271
1386-1425/

activities. The disorder of mitochondrial function will lead to the change of mitochondrial matrix composition, resulting to the change of its viscosity [10–15]. Therefore, it is crucial to develop an effective strategy for monitoring the mitochondrial viscosity to better understand various physiological activities and functions in cells.

The current intracellular viscosity senser is still a hot point in academic student, particularly in biochemical field. Several traditional analytical methods are developed to detect viscosity, such as chemiluminescence, capillary electrophoresis, spectrophotometry, and electrochemical. However, the above methods cannot be applied for viscosity measurement of biological systems *in situ* although they have wally universality for macro fluid detection. Till now, small-molecule fluorescent probes transmute the mainstream tool for detecting the viscosity in biological and pathology due to their high sensitivity, nondestructive detection, real-time imaging, and so on [16–21]. Additionally, near-infrared (NIR) fluorescent dyes are becoming effective means to monitor the level of biological indicators in cells and organisms due to its low background, high penetration depth and other advantages [22–27]. Recently, several fluorescent probes for monitoring endocellular viscosity changes have been reported (**Table S3, ESI**) [28–34]. Undeniably, most of them have excellent optical and biological properties but complex structure and difficult to be synthesized [35,36]. Therefore, a new simple and easy-to-do design idea of red emitting fluorescent probe is proposed in this paper, which seems to be a decent point.

We herein synthesized a new near-infrared fluorescent probe (**HVM**) by using 4-Dimethylaminobenzaldehyde and modified quinoline as a donor and an acceptor respectively, to distinguish normal and inflammatory models by viscosity variation with minimal background fluorescence and immense response multiples (Scheme 1). **HVM** hold an emission maximum at 670 nm and large stokes shift (160 nm). In addition, the biological imaging experiments result confirmed the ability of **HVM** was not only possesses mitochondrial targeting capability, but also has excellent membrane permeability, and can high-speed enter mitochondria in a short space of time. Thus, by way of the probe **HVM**, detected viscosity anomalous in living cells, zebrafish and mice, based on the low background fluorescence, good biocompatibility and high sensitivity of the probe. Besides, the probe **HVM** constructed in this work was potential to portray the curve of micro viscosity configuration *in vivo*.

2. Experimental section

2.1. Apparatus and chemicals

Unless otherwise mentioned, the reagents and drugs used in this paper are purchased. In addition, details of the instruments used were reviewed in the supporting literature.

2.2. Synthesis of the trans-form of *HVM* and *IVM*

HVM ((E)-4-(4-(dimethylamino)styryl)-1-ethylquinolin-1-ium iodide) and **IVM** ((E)-4-(4-(diphenylamino)styryl)-1-ethylquinolin-1-ium iodide) were synthesized according to the methods used in previous studies [37,38]. Compounds **1** (296 mg, 1 mmol), 4-Dimethylaminobenzaldehyde (149 mg, 1 mmol) or 4-(N, N-Diphenylamino) benzaldehyde (273 mg, 1 mmol) were dissolved in 8 mL alcohol with two drops of piperidine. The mixture was kept stirring vigorously for 12 h at ambient temperature, and then the solvent of the reaction mixture was removed under pressure. The crude product was purified by silica column chromatography to obtain the desired product.

HVM (258 mg, yield 60%). ^{1}H NMR (500 MHz, DMSO d_6) δ 9.17 (d, J = 5.9 Hz, 1H), 9.02 (d, J = 8.1 Hz, 1H), 8.43(d, J = 8.5 Hz, 1H),8.36 (d, J = 5.9 Hz, 2H), 8.20–8.16 (m, 2H), 8.04–7.92 (m, 2H), 7.86(d, J = 7.9 Hz, 2H), 6.80 (d, J = 7.9 Hz, 2H), 4.92 (d, J = 6.5 Hz, 3H), 3.06(s, 6H), ^{13}C NMR (126 MHz, DMSO d_6) δ 153.69, 146.26, 145.32, 138.10, 135.20, 131.86, 129.00, 127.20, 126.55, 123.5, 119.17, 114.76, 113.57, 112.33, 51.86, 40.57, 40.54, 40.37, 40.20, 40.03. HRMS(m/z): $[M]^+$ calcd for $C_{21}H_{23}N_2^+$:303.1861; found, 303.1857.

IVM (221 mg, yield 40%). ^{1}H NMR (500 MHz, DMSO d_6) δ 9.32(d, J = 6.6 Hz, 1H), 9.06–8.98 (m, 1H), 8.52 (d, J = 8.9 Hz, 1H), 8.47 (d, J = 6.7 Hz, 1H), 8.26–8.21 (m, 1H), 8.16 (d, J = 3.3 Hz), 8.03–7.99 (m, 1H), 7.90(d, J = 8.8 Hz, 2H), 7.44–7.37 (m, 4H), 7.21–7.12 (m, 6H), 6.97 (d, J = 8.8 Hz, 2H), 3.34 (s, 3H). ^{13}C NMR (126 MHz, DMSO d_6) δ 153.35, 150.29, 147.20, 146.56, 143.54, 138.13, 135.48, 131.07, 130.34, 129.39, 128.88, 127.20, 126.97, 125.96, 125.13, 120.90, 119.44, 117.35, 116.17, 40.71, 40.01, 39.78, 39.61, 39.51. HRMS (m/z): $[M]^+$ calcd for $C_{31}H_{27}N_2^+$:427.2174; found, 427.2160.

3. Results and discussion

3.1. Design and synthesis of *HVM* and *IVM*

The excogitation of viscosity probes is usually including two key factors: molecular rotor and push–pull electronic structure. Quinoline derivatives are attracted much attention in recent years because of their wide range of biological activities, excellent photophysical properties, and significant effect in organic synthesis and therapeutic chemistry [39,40]. Thus, Quinoline derivatives with the ability to target mitochondria were selected as receptor of probe. Besides, we presumed that increasing the molecular rotor might change the fluorescence properties of the fluorophores. Based on this idea, we utilized two similar structure moieties, 4-(Dimethylamino) benzaldehyde and 4-(N, N-Diphenylamino) benzaldehyde (Scheme 2), to structure different viscosity probes **HVM** and **IVM**, and discuss the trend of its fluorescence intensity with the quantity of molecular rotors. When the probe was in non-viscosity or low viscosity environment, the molecular rotates rotors freely around the single bond, resulting the probe intermolecular energy nonradiative (Scheme 1). With the increase of viscosity, the rotation of molecules was limited, which turned on

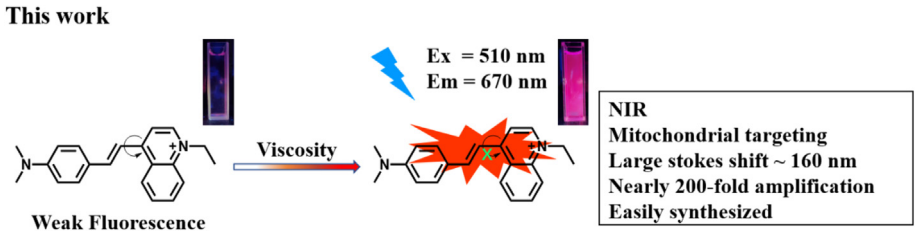

Scheme 1. The design strategy of **HVM** response to viscosity.

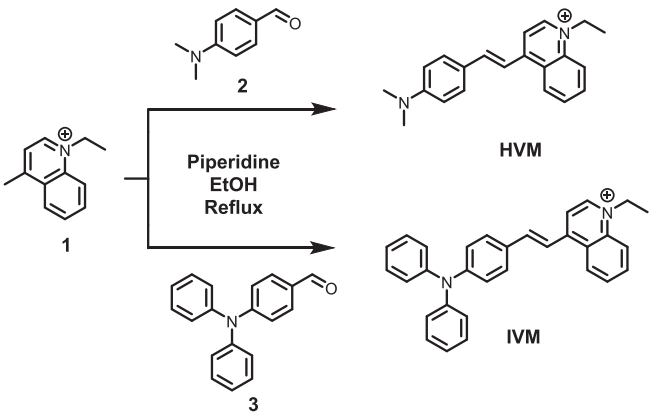

Scheme 2. Synthesis of the *trans*-form of **HVM** and **IVM**.

the red fluorescence signal. The structures of **HVM** and **IVM** were ample characterized by ^{1}H and ^{13}C NMR spectroscopy and HRMS (high resolution mass spectrometer) (Fig. S6-S10).

3.2. Optical properties of *HVM* and *IVM*

Primarily, the optical responded capability of **HVM** and **IVM** to the viscosity was evaluated by absorption and fluorescence spectra in PBS solution-glycerol system. From the ultraviolet absorption spectra, we found that the maximum absorption peaks of **HVM** and **IVM** were red shifted about 40 nm (510–550 nm) and 30 nm (500–530 nm) from PBS buffer solution to glycerol system, respectively (Fig. 1a, 1d). Compared with **HVM**, the absorption peak of **IVM** with two benzene rings in the aniline part blue-shifted slightly. This phenomenon may be caused by the increase of the number of molecular rotors, which makes the conjugation system of the probe relatively weak. Furthermore, the fluorescence spectra of **HVM** and **IVM** were measured by adjusting PBS solution and glycerol system with different viscosity gradients under the same parameters. It was found that the fluorescence intensity increased with the increase of viscosity (Fig. 1b, 1e). In addition, the results show that the fluorescence enhancement of **HVM** was about 195-fold, significantly higher than that of **IVM** (147-fold) under the same condition. Similar to the above results, the linear relationship of **HVM** was also superior to that of **IVM**(Fig. 1c, 1f). At the same time, the fluorescence quantum yields of the two compounds were calculated, and the results showed that the fluorescence quantum yields of **HVM** (174-fold) were also significantly enhanced than that of **IVM** (75-fold) (Table. S2 ESI). These experimental results showed that **HVM** had better optical properties and viscosity response compared with **IVM**, so **HVM** was selected for further researches.

Afterwards, the selectivity of probe **HVM** to various related species in organism was detected. Metal ions, anions and active small molecules were used as typical species to verify the selectivity of **HVM** in complex biological microenvironment (Fig. 2a, Table. S3, ESI). All the interference species (1 mM) that could be considered induce almost negligible fluorescence changes in PBS buffer solution. This further indicated that **HVM** could be used to detect intracellular viscosity. In order to further study the biological application ability of the probe, we simulated the viscosity microenvironment of mitochondria *in vivo* and detected the fluorescence intensity of **HVM** in the presence of different interfering ions (Fig. 3a). As we expected, **HVM** was barely affected by the necessary species for regulating life activities. This was consistent with the previous selectivity results, indicated that the probe had classy anti-interference ability and suitable for monitoring mitochondrial viscosity.

Specificity and stability of probes were basic and key for biological applications, which were particularly important in viscosity detection. Before that, we first studied the effect of different solvents on the probe, and the results showed that there was a weak fluorescence signal in different solvents of **HVM** compared with glycerol. It was also drawing a conclusion that the solvent had little effect on the fluorescence emission of probe **HVM** (Fig. S2a, S2b, ESI). In addition, the effect of pH on **HVM** was investigated in PBS solution and 50% glycerol solution (PBS: glycerol = 1:1) of different pH (Fig. 2b). The results showed that the fluorescence intensity of the probe changed little in the two different systems in the pH range of 4.01 ~ 10.07. Furthermore, we explored the excellent optical properties of **HVM** by evaluating its photobleaching resistance (Fig. 3b). The results showed that the fluorescence intensity

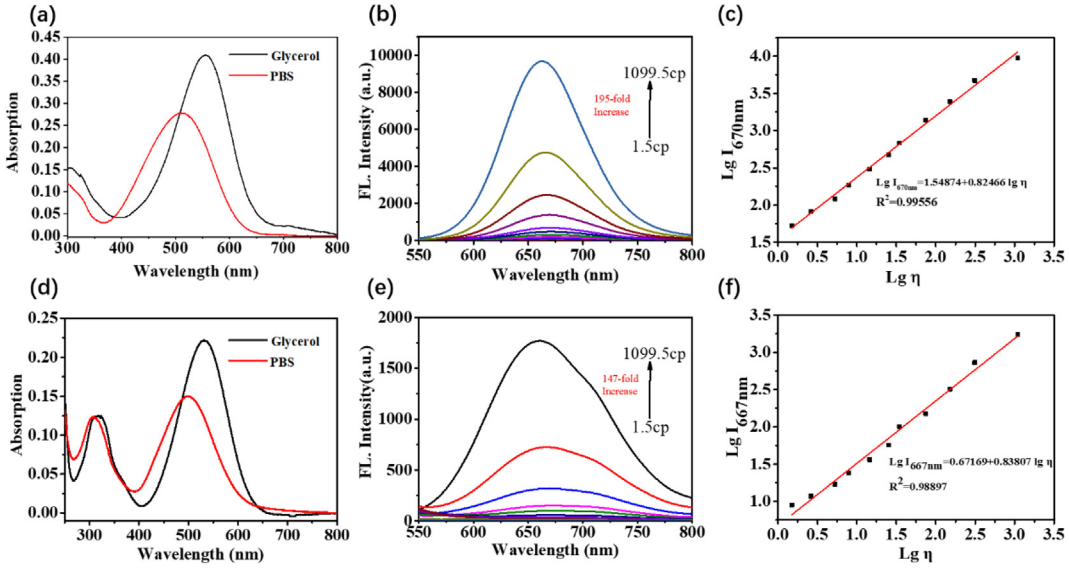

Fig. 1. (a, d) Absorption of probe **HVM** (a) and **IVM** (d) (10 μM) in glycerol solution (black line) and PBS solution (red line); (b, e) Fluorescence changes of **HVM** (λ_{ex} = 510 nm) (b) and **IVM** (λ_{ex} = 500 nm) (e) in PBS–glycerol solution with different viscosities (1.5–1099.5 cP), Excitation Slit: 20.0 nm, Emission Slit: 20.0 nm; (c, f) Curve plotted with lg (I_{670nm}) versus lg (η) of **HVM** (c) and **IVM** (f).

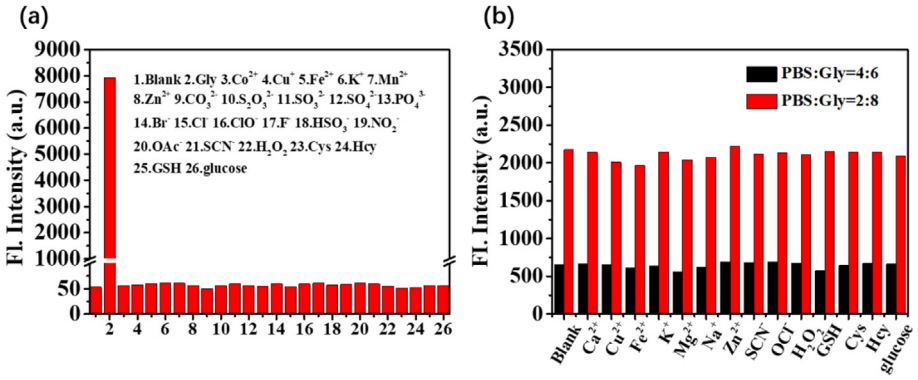

Fig. 2. (a) The fluorescence intensity of **HVM** (10 μM) in glycerol or in PBS solution with the various anions (1 mM). (b) The fluorescence intensity of **HVM** (10 μM) treated with various species (1 mM) in mixtures of glycerol and PBS at different ratios: blank; Ca^{2+}; Cu^{2+}; Fe^{2+}; K^{+}; Mg^{2+}; Na^{+}; Zn^{2+}; SCN^{-}; OCl^{-}; H_2O_2; Cys; Hcy; GSH; glucose. $\lambda_{ex/em}$ = 510/670 nm, Excitation Slit: 20.0 nm, Emission Slit: 20.0 nm.

of **HVM** probe remained unchanged with the increase of illumination time (60 min) in several commonly used solvents, which indicated that **HVM** had excellent photobleaching boycott. Through the above experiments, **HVM** had Excellent pH reliability and optical stability, and these experimental data provided the basis for further research.

3.3. Fluorescence imaging in living cells

Before the biological application experiment, we first analyzed the biological toxicity of **HVM** as a pre-index to the HeLa cells by MTT assays (Fig. S5, ESI). The results showed that the survival rate of HeLa cells was 85% at the probe concentration reached 50 μM. This indicated that **HVM** had negligible cytotoxicity, and it could be used in the future biological scientific study. Moreover, it was necessary to evaluated the cellular localization and potential application capacity of **HVM**. We observed the staining of cells under confocal microscope, and the **HVM** probe could penetrate into cells in a short incubation period (1 min) and showed the strongly fluorescence signal. To verify the ability to target mitochondria of **HVM**, the cells were stained **HVM** (10 μM) and Mitochondrial Deep Red FM (500 nM) together (Fig. 4a and 4b). The combined image showed that red fluorescence and purple fluorescence overlaps well (Fig. 4c). Then the probe with a high Pearson's correlation of 0.92 was confirmed by the intensity scatter plot and the intensity profile of the two channels (Fig. 4d, 4e). Hence, colocalization results showed that **HVM** primarily assembled in the mitochondria.

To validate that **HVM** was sensitive to abnormal change viscosity, fluorescence images of HeLa cells were obtained in the presence ionophores of monensin (Mon) and nystatin (Ny) [41,42]. As stimulants of cell state, Mon and Ny can induce the change or expansion of mitochondrial structure, bringing about mitochondrial viscosity increase. To eliminate the interference of Mon and Ny, the fluorescence spectra of ionophores were determined before cell imaging (Fig. S3, ESI). The results showed that the fluorescence intensity of **HVM** remained unchanged with around stimulus imputed, indicated that **HVM** could be effectively applied to monitor cell viscosity and related *in vivo* studies. To evaluate the effectiveness of **HVM** in intracellular viscosity imaging, we obtained confocal images of HeLa cells loaded with **HVM** probe after treating two kinds of ionophores. From the Fig. 5a1-a3, the cells treated with **HVM** merely showed weak red fluorescence. In contrast, HeLa cells treated with Mon (Fig. 5b1-b3) or Ny (Fig. 5c1-c3) showed exceedingly shining red fluorescence. Meanwhile, this result can be observed more intuitively by image quantization, and the fluorescence intensity increases about 3–4 times before and after cell stimulation (Fig. 5d). Therefore, this experiment showed that **HVM** had a classy effect for the monitoring of cell viscosity changes.

3.4. Monitoring viscosity in zebrafish

We have certificated that the probe **HVM** can visualize the change of cell viscosity, therefore, **HVM** viscosity imaging in zebrafish was further studied. In the initial study, we incubated zebrafish for 30 min with **HVM** (Fig. 6a1-a3), and the weak red fluorescence signal could be observed. After that, the viscosity of zebrafish was increased by drug stimulation (Mon and Ny), and incubated with **HVM** for the same time. Compared with simplex probe handle, the

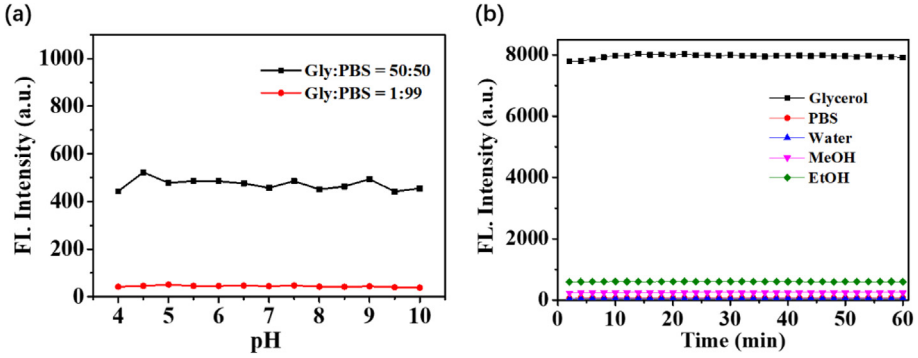

Fig. 3. (a) The fluorescence intensity of **HVM** (10 μM) in PBS (red) or in glycerol: PBS = 1:1 (black) at different pH. (b) The photostability of **HVM** in glycerol, PBS, water, MeOH and EtOH with continuous irradiation for 60 min. $\lambda_{ex/em}$ = 510/670 nm, Excitation Slit: 20.0 nm, Emission Slit: 20.0 nm.

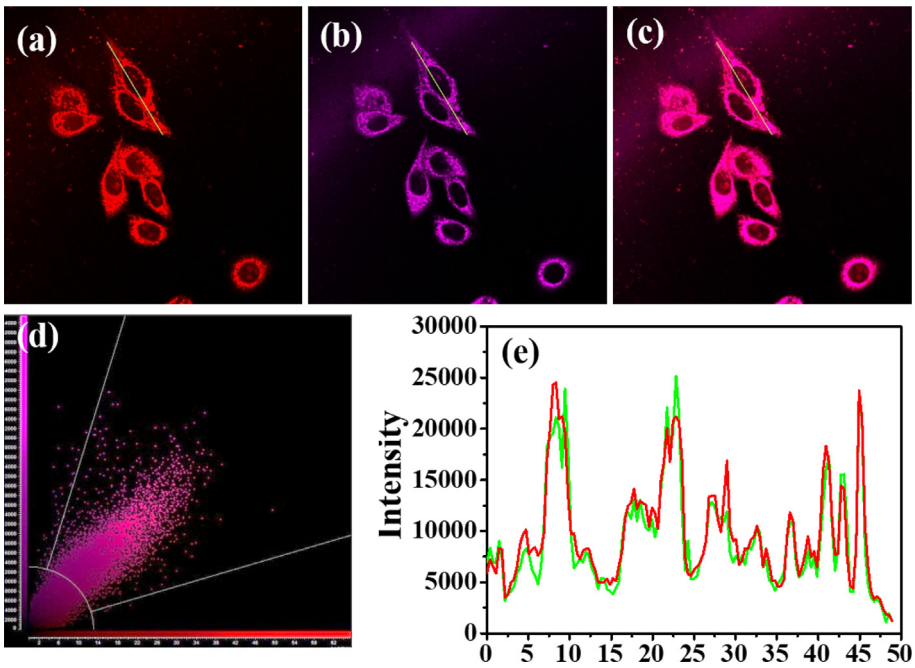

Fig. 4. Co-stained fluorescence images of **HVM** in HeLa cells. The cells were stained with (a) Mito-targeting Deep Red and (b) **HVM**. Mito-targeting Deep Red: λ_{ex} = 644 nm, λ_{em} = 655–675 nm; **HVM**: λ_{ex} = 510 nm, λ_{em} = 640–700 nm. (c) Merged image of (a) and (b). (d) Intensity scatter plots of the probe **HVM** across the cells in the red and purple channels. (e) Intensity profile of the two channels.

fluorescence signal intensity of zebrafish was significantly enhanced after drug treatment (Fig. 6b1-b3 and c1-c3). Similarly, data of comparison showed that the fluorescence intensity ascend by 2–3 times (Fig. 6d). Significantly, the above experimental results were basically consistent with the cells imaging experiment, and the sterling biological properties of the probe prompted us to further study.

3.5. Fluorescence imaging in normal and inflammation living mice models

Based on the ideal results obtained, we further explored its fluorescent map by constructing inflammation models compared with normal mice. Lipopolysaccharide (LPS), Mon and Ny were injected into different mice to construct multiple disease models [43]. After that, **HVM** was added to normal mice and inflammatory mice for imaging experiment (Fig. 7a-d). Obvious change of fluorescence signal could be observed, and the fluorescence intensity of mice with inflammation model was significantly higher than normal mice. These results were consistent with the cell level and zebrafish imaging, indicated the probe **HVM** can distinguish the abnormal changes of viscosity *in vivo*. In a few words, the probe **HVM** not only detected the viscosity but also furnished a concise tactic for diagnoses of viscosity-related diseases.

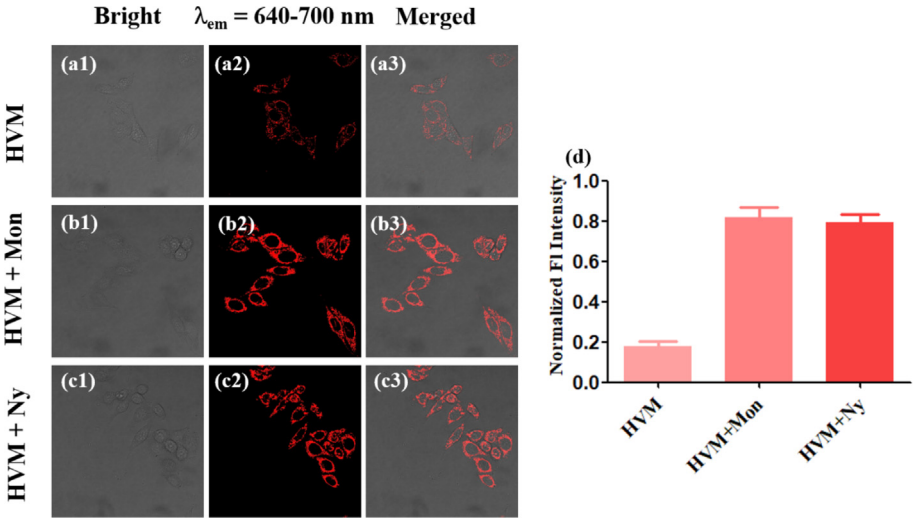

Fig. 5. (a1–a3) Fluorescence imaging in HeLa cells cultured with 5 μM **HVM**. (b1–b3) Fluorescence imaging in HeLa cells cultured with 5 μM Monensin for 30 min and 5 μM **HVM** for an additional 10 min. (c1–c3) Fluorescence imaging in HeLa cells cultured with 5 μM Nystatin for 30 min and 5 μM **HVM** for an additional 10 min. (d) Normalized fluorescence intensity of HeLa cells. λ_{ex} = 510 nm, λ_{em} = 640–700 nm.

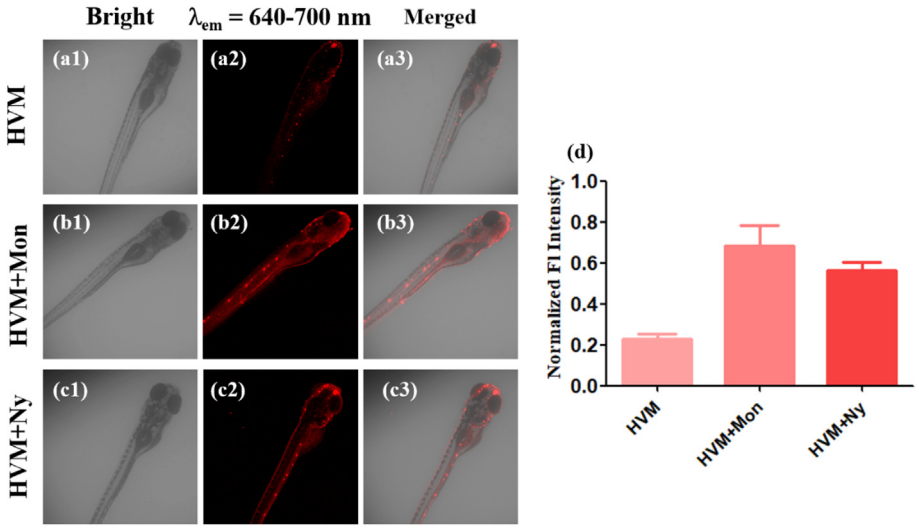

Fig. 6. (a1–a3) Fluorescence imaging in zebrafish cultured with 5 μM **HVM**. (b1–b3) Fluorescence imaging in zebrafish cultured with 5 μM Monensin for 30 min and 5 μM **HVM** for an additional 30 min. (c1–c3) Fluorescence imaging in zebrafish cultured with 5 μM Nystatin for 30 min and 5 μM **HVM** for an additional 30 min. (d) Normalized fluorescence intensity of HeLa cells. Conditions: λ_{ex} = 510 nm, λ_{em} = 640–700 nm.

4. Conclusion

In summary, we have proposed a novel NIR fluorescent probe **HVM** with a small-molecule weight of mitochondrial-trackable to discriminate normal and inflammatory models. **HVM** displayed high stability, specific selectivity, ultrahigh sensitivity, low cytotoxicity and beneficial biocompatibility. We employed it to image the viscosity of mitochondria in living HeLa cells. The results showed that compared with untreated cells, the viscosity of mitochondria increased significantly after drug stimulation. Besides, based on the excellent properties of the probe, **HVM** was proven to further monitor the increased viscosity in zebrafish and mice. These findings indicated that this simple near-infrared fluorescent probe provides a powerful tool for studying the relationship between disease and viscosity in the realms of biology and medicine.

CRediT authorship contribution statement

Chen Geng: Conceptualization, Investigation, Methodology, Project administration, Data curation, Formal analysis, Software, Writing – original draft, Writing – review & editing. **Jingting Zhan:**

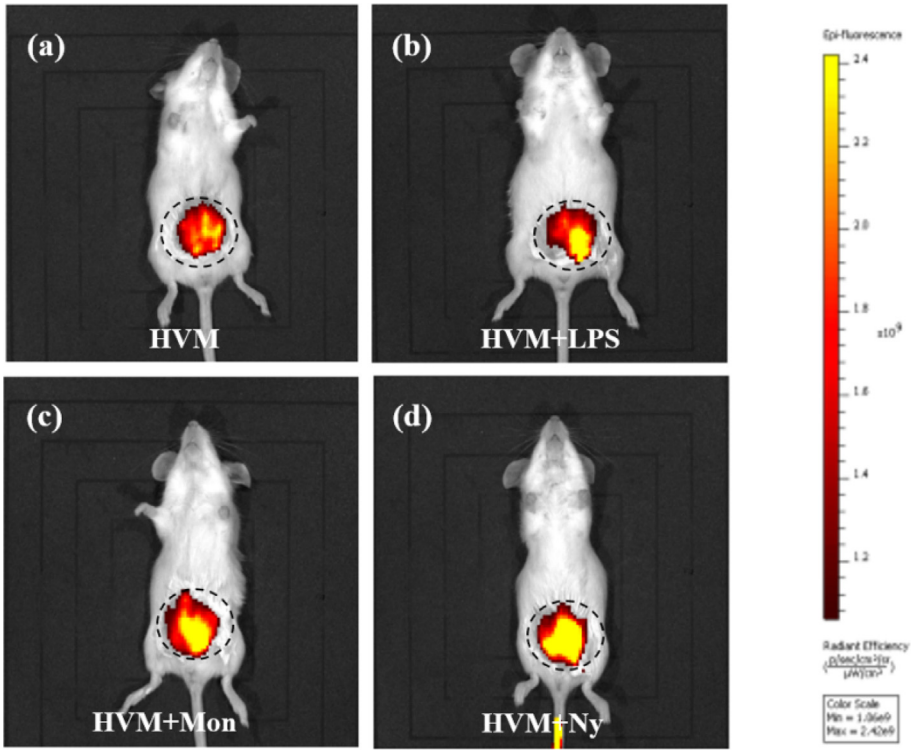

Fig. 7. Fluorescence imaging of normal living mice (a), mice induced with LPS (b), monensin (c), and nystatin (d) injected 100 μL **HVM** (1 mM). λ_{ex} = 520 nm, λ_{em} = 650 nm.

Conceptualization, Methodology, Formal analysis, Validation, Visualization, Writing – review & editing. **Xinya Hao:** Investigation, Resources, Visualization. **Wenhui Song:** Investigation, Resources, Validation, Visualization. **Weiying Lin:** Resources, Funding acquisition, Supervision, Writing – review & editing.

Declaration of Competing Interest

The authors declare that they have no known competing financial interests or personal relationships that could have appeared to influence the work reported in this paper.

Acknowledgements

This work was financially supported by the National Natural Science Foundation of China (21672083, 21877048, 22077048), Guangxi Natural Science Foundation (2020JJD120023), and the startup fund of Guangxi University (A3040051003).

Appendix A. Supplementary data

Supplementary data to this article can be found online at https://doi.org/10.1016/j.saa.2021.120271.

References

[1] J.H. Hong, M.S. Ko, P.S. Rao, D.G. Cho, Systematic Modifications of a Simple Tolan: Another Category of Viscosity Sensor, Org. Lett. 21 (2019) 10085–10089.
[2] C. Trapnell, B.A. Williams, G. Pertea, A. Mortazavi, G. Kwan, M.J. van Baren, S.L. Salzberg, B.J. Wold, L. Pachter, Transcript assembly and quantification by RNA-Seq reveals unannotated transcripts and isoform switching during cell differentiation, Nat. Biotechnol. 28 (5) (2010) 511–515.
[3] Y. Zhang, Z. Li, W. Hu, Z. Liu, A Mitochondrial-Targeting Near-Infrared Fluorescent Probe for Visualizing and Monitoring Viscosity in Live Cells and Tissues, Anal. Chem. 91 (15) (2019) 10302–10309.
[4] H. Chen, Y. Tang, H. Shang, X. Kong, R. Guo, W. Lin, Development of a unique family of two-photon full-color-tunable fluorescent materials for imaging in live subcellular organelles, cells, and tissues, J. Mater. Chem. B 5 (13) (2017) 2436–2444.
[5] D. Han, J. Yi, C. Liu, L. Liang, K. Huang, L. Jing, D. Qin, A fluoran-based viscosity probe with high-performance for lysosome-targeted fluorescence imaging, Spectrochim. Acta - Part A Mol. Biomol. Spectrosc. 238 (2020) 118405.
[6] J. Yin, M. Peng, W. Lin, Visualization of Mitochondrial Viscosity in Inflammation, Fatty Liver, and Cancer Living Mice by a Robust Fluorescent Probe, Anal. Chem. 91 (13) (2019) 8415–8421.
[7] Z. Yang, Y. He, J.-H. Lee, N. Park, M. Suh, W.-S. Chae, J. Cao, X. Peng, H. Jung, C. Kang, J.S. Kim, A self-calibrating bipartite viscosity sensor for mitochondria, J. Am. Chem. Soc. 135 (24) (2013) 9181–9185.
[8] J.A. Robson, M. Kubánková, T. Bond, R.A. Hendley, A.J.P. White, M.K. Kuimova, J. D.E.T. Wilton-Ely, Simultaneous Detection of Carbon Monoxide and Viscosity Changes in Cells, Angew. Chemie - Int. Ed. 59 (48) (2020) 21431–21435.
[9] M.K. Kuimova, G. Yahioglu, J.A. Levitt, K. Suhling, Molecular rotor measures viscosity of live cells via fluorescence lifetime imaging, J. Am. Chem. Soc. 130 (21) (2008) 6672–6673.
[10] S.-H. Park, I. Shin, Y.-H. Kim, I. Shin, Mitochondrial Cl–Selective Fluorescent Probe for Biological Applications, Anal. Chem. 92 (18) (2020) 12116–12119.
[11] M. Ren, K. Zhou, L. Wang, K. Liu, W. Lin, Construction of a ratiometric two-photon fluorescent probe to monitor the changes of mitochondrial viscosity, Sensors Actuators, B Chem. 262 (2018) 452–459.
[12] L. Hao, Z.W. Li, D.Y. Zhang, L. He, W. Liu, J. Yang, C.P. Tan, L.N. Ji, Z.W. Mao, Monitoring mitochondrial viscosity with anticancer phosphorescent Ir(iii) complexes: Via two-photon lifetime imaging, Chem. Sci. 10 (2019) 1285–1293.
[13] C.D.L. Folmes, P.P. Dzeja, T.J. Nelson, A. Terzic, Mitochondria in control of cell fate, Circ. Res. 110 (4) (2012) 526–529.
[14] J. Cheng, Z. Li, W. Lin, Development of a one-step synthesized red emission fluorescent probe for sensitive detection of viscosity in vitro and in vivo, Spectrochim. Acta - Part A Mol. Biomol. Spectrosc. 258 (2021) 119808.
[15] J. Yang, R. Zhang, Y. Zhao, J. Tian, S. Wang, C.P. Gros, H. Xu, Red/NIR neutral BODIPY-based fluorescent probes for lighting up mitochondria, Spectrochim. Acta - Part A Mol. Biomol. Spectrosc. 248 (2021) 119199, https://doi.org/10.1016/j.saa.2020.119199.
[16] Z. Yang, J. Cao, Y. He, J.H. Yang, T. Kim, X. Peng, J.S. Kim, Macro-/micro-environment-sensitive chemosensing and biological imaging, Chem. Soc. Rev. 43 (13) (2014) 4563–4601.
[17] M.A. Haidekker, T.P. Brady, D. Lichlyter, E.A. Theodorakis, A ratiometric fluorescent viscosity sensor, J. Am. Chem. Soc. 128 (2) (2006) 398–399.
[18] Z. Yang, J. Fan, X. Peng, Fluorescence ratiometry and fluorescence lifetime (FLIM) imaging: Dual mode imaging cellular viscosity by a single molecular rotor, 2011 Funct, Opt. Imaging, FOI (2011, 2011,) 6626–6635.
[19] S. Ye, H. Zhang, J. Fei, C.H. Wolstenholme, X. Zhang, A General Strategy to Control Viscosity Sensitivity of Molecular Rotor-Based Fluorophores, Angew. Chemie - Int. Ed. 60 (3) (2021) 1339–1346.
[20] J. Gonzalez-Molina, X. Zhang, M. Borghesan, J. Mendonça da Silva, M. Awan, B. Fuller, N. Gavara, C. Selden, Extracellular fluid viscosity enhances liver cancer cell mechanosensing and migration, Biomaterials 177 (2018) 113–124.
[21] H.-y. Tan, Y.-T. Qiu, H. Sun, J.-w. Yan, L. Zhang, A lysosome-Targeting dual-functional fluorescent probe for imaging intracellular viscosity and beta-Amyloid, Chem. Commun. 55 (18) (2019) 2688–2691.
[22] A. Zheng, H. Liu, X. Gao, K. Xu, B. Tang, A Mitochondrial-Targeting Near-Infrared Fluorescent Probe for Revealing the Effects of Hydrogen Peroxide And Heavy Metal Ions on Viscosity, Anal. Chem., 2021.
[23] X.-Z. Yang, B. Xu, L. Shen, R.u. Sun, Y.-J. Xu, Y.-L. Song, J.-F. Ge, Series of Mitochondria/Lysosomes Self-Targetable Near-Infrared Hemicyanine Dyes for Viscosity Detection, Anal. Chem. 92 (5) (2020) 3517–3521.
[24] Y.N. Wang, B. Xu, L.H. Qiu, R. Sun, Y.J. Xu, J.F. Ge, Viscosity sensitive fluorescent dyes with excellent photostability based on hemicyanine dyes for targeting cell membrane, Sensors Actuators, B Chem. 337 (2021) 129787.
[25] J. Ning, T. Liu, P. Dong, W. Wang, G. Ge, B.o. Wang, Z. Yu, L. Shi, X. Tian, X. Huo, L. Feng, C. Wang, C. Sun, J. Cui, T.D. James, X. Ma, Molecular Design Strategy to Construct the Near-Infrared Fluorescent Probe for Selectively Sensing Human Cytochrome P450 2J2, J. Am. Chem. Soc. 141 (2) (2019) 1126–1134.
[26] M. Cui, M. Ono, H. Watanabe, H. Kimura, B. Liu, H. Saji, Smart near-infrared fluorescence probes with donor-acceptor structure for in vivo detection of β-amyloid deposits, J. Am. Chem. Soc. 136 (9) (2014) 3388–3394.
[27] W. Mazi, Y. Yan, Y. Zhang, S. Xia, S. Wan, M. Tajiri, R.L. Luck, H. Liu, A near-infrared fluorescent probe based on a hemicyanine dye with an oxazolidine switch for mitochondrial pH detection, J. Mater. Chem. B 9 (3) (2021) 857–863.
[28] M. Ren, B. Deng, K. Zhou, X. Kong, J.-Y. Wang, W. Lin, Single Fluorescent Probe for Dual-Imaging Viscosity and H2O2 in Mitochondria with Different Fluorescence Signals in Living Cells, Anal. Chem. 89 (1) (2017) 552–555.
[29] L. Zhu, M. Fu, B. Yin, L. Wang, Y. Chen, Q. Zhu, A red-emitting fluorescent probe for mitochondria-target microviscosity in living cells and blood viscosity detection in hyperglycemia mice, Dye. Pigment. 172 (2020) 107859.
[30] Y. Ma, Y. Zhao, R. Guo, L. Zhu, W. Lin, A near-infrared emission fluorescent probe with multi-rotatable moieties for highly sensitive detection of mitochondrial viscosity in an inflammatory cell model, J. Mater. Chem. B 6 (39) (2018) 6212–6216.
[31] Y. Baek, S.J. Park, X. Zhou, G. Kim, H.M. Kim, J. Yoon, A viscosity sensitive fluorescent dye for real-time monitoring of mitochondria transport in neurons, Biosens. Bioelectron. 86 (2016) 885–891.
[32] Z. Zou, Q.i. Yan, S. Ai, P. Qi, H. Yang, Y. Zhang, Z. Qing, L. Zhang, F. Feng, R. Yang, Real-Time Visualizing Mitophagy-Specific Viscosity Dynamic by Mitochondria-Anchored Molecular Rotor, Anal. Chem. 91 (13) (2019) 8574–8581.
[33] Y. Li, D. Xu, S.L. Ho, H.W. Li, R. Yang, M.S. Wong, A theranostic agent for in vivo near-infrared imaging of β-amyloid species and inhibition of β-amyloid aggregation, Biomaterials 94 (2016) 84–92.
[34] J. Xu, Y. Zhang, H. Yu, X. Gao, S. Shao, Mitochondria-Targeted Fluorescent Probe for Imaging Hydrogen Peroxide in Living Cells, Anal. Chem. 88 (2) (2016) 1455–1461.
[35] M. Tian, Y. Ma, W. Lin, Fluorescent Probes for the Visualization of Cell Viability, Acc. Chem. Res. 52 (8) (2019) 2147–2157.
[36] Y. Tang, Y. Ma, J. Yin, W. Lin, Strategies for designing organic fluorescent probes for biological imaging of reactive carbonyl species, Chem. Soc. Rev. 48 (15) (2019) 4036–4048.
[37] L.N. Schulte, B. Heinrich, H. Janga, B.T. Schmeck, O. Vázquez, A Far-Red Fluorescent DNA Binder for Interaction Studies of Live Multidrug-Resistant Pathogens and Host Cells, Angew. Chemie - Int. Ed. 57 (36) (2018) 11564–11568.
[38] N. Gupta, S.I. Reja, V. Bhalla, M. Gupta, G. Kaur, M. Kumar, A bodipy based fluorescent probe for evaluating and identifying cancer, normal and apoptotic C6 cells on the basis of changes in intracellular viscosity, J. Mater. Chem. B 4 (11) (2016) 1968–1977.
[39] Y.F. Wei, X.F. Weng, X.L. Sha, R. Sun, Y.J. Xu, J.F. Ge, Simultaneous imaging of lysosomal and mitochondrial viscosity under different conditions using a NIR probe, Sensors Actuators, B Chem. 326 (2021) 128954.
[40] X. Yan, L. Ge, M. Castiñeira Reis, S.R. Harutyunyan, Nucleophilic Dearomatization of N-Heteroaromatics Enabled by Lewis Acids and Copper Catalysis, J. Am. Chem. Soc. 142 (47) (2020) 20247–20256.
[41] J.A. Pizzey, F.A. Bennett, G.E. Jones, Monensin inhibits initial spreading of cultured human fibroblasts, Nature 305 (5932) (1983) 315–317.
[42] M. Tester, Membrane Biology 9, J. Membr. Biol. 103 (1988) 159–170.
[43] S. Shen, F. Han, A. Yuan, L. Wu, J. Cao, J. Qian, X. Qi, Y. Yan, Y. Ge, Engineered nanoparticles disguised as macrophages for trapping lipopolysaccharide and preventing endotoxemia, Biomaterials 189 (2019) 60–68.